Adsorption (2008) 14: 601–610
DOI 10.1007/s10450-008-9111-3

Adsorption of mercury from single and multicomponent metal systems on activated carbon developed from cherry stones

M. Olivares-Marín · C. Fernández-González ·
A. Macías-García · V. Gómez-Serrano

Received: 27 April 2007 / Revised: 7 February 2008 / Accepted: 11 February 2008 / Published online: 5 March 2008

Abstract The adsorption of mercury from a single/multisolute aqueous solution by activated carbon (AC) prepared from cherry stones (CS) by chemical activation with H_3PO_4, $ZnCl_2$ or KOH is studied. Three series of AC (i.e., P, H_3PO_4; Z, $ZnCl_2$; K, KOH) were prepared by controlling the impregnation ratio and carbonization temperature. The textural characterization of AC was carried out by gas adsorption, mercury porosimetry and density measurements. The surface chemistry was analyzed by the pH of the point of zero charge (pH_{zpc}), FT-IR spectroscopy and Boehm's method. Experiments of mercury adsorption were conducted by the batch method, using aqueous solutions of mercury and of mercury, cadmium and zinc without pH adjustment. The ACs possess a wide range of pore volumes and sizes. Their microporosity is usually well developed. The meso- and macropore volumes are higher for the P carbons and K carbons, respectively. BET surface areas as a rule range between 1000 and 2000 $m^2\ g^{-1}$. The pH_{zpc} is much lower for the P carbons. The content of acidic oxygen surface groups is lower for the K carbons, whereas the content of basic groups is higher for these carbons. The kinetics of the adsorption process of mercury is faster for ACs with high volumes of large size pores. However, the surface groups have a marked unfavorable influence on the kinetics. The pseudo-second order rate constant ($k_2 \times 10^{-3}$, g/mol h) is higher by the order Z-4-800 (67.69) > K-3-800 (43.45) > P-3.44-400 (36.98). The incorporation of zinc and cadmium to the mercury solution usually decelerates the adsorption process for the P carbons and Z carbons and accelerates it for the K carbons. The amount adsorbed of mercury is much larger for the K carbons than for the other ACs. For the Z carbons, competition effects of zinc and cadmium on the adsorption of mercury are negligible, which indicates that mercury adsorbs specifically on surface active sites of these adsorbents.

Keywords Cherry stones · Activated carbon · Mercury adsorption

1 Introduction

Mercury has been well known as an environmental pollutant for several decades. Both mercury and its compounds have high acute and chronic toxicity on aquatic life, even at low concentrations (Zelikoff and Thomas 2005). Municipal landfills, sewage, metal refining, and chemical manufacturing are significant potential emitters of mercury to land and water. In the environment, mercury is found in its elemental form and in various organic compounds and complexes. One of the most toxic mercury chemical species is mercury dichloride ($HgCl_2$) because this substance easily forms organomercury complexes with proteins (Clarkson 2002). In general, for the reduction of mercury from wastewater several technologies such as sulfide precipitation, ion exchange, alum and iron coagulation, electro deposition and adsorption process have been developed (Zhang et al. 2005). Of these technologies adsorption by activated carbon (AC) is the most attractive process, primarily due to

---

M. Olivares-Marín · C. Fernández-González ·
V. Gómez-Serrano (✉)
Departamento de Química Orgánica e Inorgánica,
Facultad de Ciencias, Universidad de Extremadura,
Avda. de Elvas s/n, 006071 Badajoz, Spain
e-mail: vgomez@unex.es

A. Macías-García
Área de Ciencia de Materiales, Escuela de Ingenierías
Industriales, Universidad de Extremadura, Avda. de Elvas s/n,
006071 Badajoz, Spain

the low production cost of this material and to its high effectiveness. AC is a porous carbonaceous material that possesses high adsorptive capacities associated with its exceptional physical-chemical properties. These properties, which include not only the porous structure but also the surface chemistry, depend on the starting material and the method used in its preparation. Cheap materials with a high carbon content and low in inorganics are used as raw material for the production of AC (Bansal et al. 1988). Currently, one of the activation strategies available to develop AC is the so-called method of chemical activation. This consists basically of pyrolysis of a given precursor at temperatures between 400–800 °C (Bansal et al. 1988) in the presence of a chemical activating agent which influences the course of pyrolysis. Among the activating agents used most frequently are H_3PO_4, $ZnCl_2$, KOH, etc. A wealth of literature is devoted to studies of the adsorption of mercury from a single solute solution by AC (Valenzuela Calahorro et al. 1990; Gómez-Serrano et al. 1998; Pulido et al. 1998; Hsi et al. 2002; Yardim et al. 2003; Li et al. 2003; Ho et al. 2004; Nabais et al. 2006; and so on). However, the use of ACs prepared by chemical activation with various activating agents has been much less frequent (Zhang et al. 2005). Also, adsorption studies of metal ions from binary or multi-component aqueous solutions by AC are rare (Pardo-Botello et al. 2004, 2005), in spite of the fact that natural and artificial aqueous systems are frequently a complex matrix of various metallic solutes. In this study, the adsorption of mercury from single solute (mercury) and multi-solute (mercury, zinc and cadmium) aqueous solutions by several ACs prepared from cherry stones (CS), which is an agricultural waste product generated in abundance by the agrarian industry in the Valle del Jerte (Cáceres province, Spain), by chemical activation with H_3PO_4, $ZnCl_2$ or KOH is investigated. Special emphasis is laid on the influence of the porous structure and surface chemistry of AC on the kinetics of the adsorption process of mercury from such aqueous solutions.

2 Experimental

2.1 Preparation and characterization of AC

Using CS (particle size, 1–2 mm) (Durán-Valle et al. 2005), three series of ACs were first prepared by chemical activation with H_3PO_4, $ZnCl_2$ or KOH. The products obtained were then characterized texturally by gas physical adsorption (N_2, −196 °C; CO_2, 0 °C), mercury porosimetry, and density measurements. Details of the methods used in the preparation and characterization of the ACs have been given in previous reports (Olivares-Marín et al. 2006a, 2006b, 2007). Table 1 lists the yield values, and series and sample codes. The textural data obtained for the ACs have been compiled in Table 2. The surface chemistry of selected ACs was analyzed by pH of the point of zero charge (pH_{zpc}) (Newcombe et al. 1993; Lopez-Ramon et al. 1999), FT-IR spectroscopy, and Boehm's method (Boehm 1966). The analysis of the ACs by FT-IR spectroscopy was carried out as described elsewhere (Gómez-Serrano et al. 1999, 2005). Using an FT-IR spectrometer, Perkin-Elmer 1720, the spectra were recorded in the range of wavenumbers 4000–400 cm^{-1}. Fifty scans were taken at 2 cm^{-1} resolution. After thoroughly mixing AC and KBr (Merck, for spectroscopy) in an agate mortar, pellets were prepared at the AC to KBr impregnation ratio 1:500. The spectrum of a KBr pellet, containing the same amount of dispersant as for the AC/BrK pellets, was used as background. The values of pH_{zpc} and contents of acidic-basic groups obtained for the analyzed ACs are given in Table 3.

2.2 Experiments of mercury adsorption

Using a suit of test tubes, which were provided with bakelite screw-on caps to avoid solvent losses, samples of ∼0.10 g for the series P and Z and of ∼0.01 g for the series K were

Table 1 Preparation of the ACs. Series and sample codes[a]

Series codes	Sample codes	Preparation			
		AA	I_R	C_T (°C)	Yield (%)
P	P-0.64-400	H_3PO_4	0.64	400	48
	P-3.44-400		3.44	400	47
	P-3.44-500		3.44	500	45
Z	Z-1-500	$ZnCl_2$	1	500	39
	Z-4-500		4	500	39
	Z-4-800		4	800	38
K	K-1-800	KOH	1	800	15
	K-3-500		3	500	20
	K-3-800		3	800	12
	K-3-900		3	900	5

[a] AA, activating agent; I_R, AA:CS impregnation ratio; C_T, carbonization temperature

Table 2 Textural characterization of the ACs

Series codes	Sample codes	Textural data						
		$S_{\text{BET-0.1}}$[a] (m^2/g)	$S_{\text{BET-0.3}}$[a] (m^2/g)	W_0 (N_2)[a] (cm^3/g)	W_0 (CO_2)[b] (cm^3/g)	V_{me}[c] (cm^3/g)	V_{ma}[c] (cm^3/g)	V_T[d] (cm^3/g)
P	P-0.64-400	1153	946	0.48	0.37	0.28	0.11	0.54
	P-3.44-400	1350	1277	0.47	0.28	0.46	0.23	0.94
	P-3.44-500	1624	1688	0.55	0.28	0.78	0.49	1.55
Z	Z-1-500	682	567	0.28	0.32	0.02	0.37	0.86
	Z-4-500	2043	1971	0.68	0.27	0.45	0.34	1.15
	Z-4-800	1389	1267	0.51	0.34	0.16	0.50	0.98
K	K-1-800	1430	1171	0.57	0.55	0.08	0.48	1.13
	K-3-500	324	279	0.13	0.24	0.00	0.87	1.21
	K-3-800	1406	1167	0.56	0.59	0.00	1.25	2.07
	K-3-900	1842	1624	0.67	0.43	0.17	1.84	2.88

[a] N_2 isotherm at −196 °C: S_{BET}, BET surface area (Brunauer et al. 1938); $S_{\text{BET-0.1}}$, $p/p^0 = 0.05$–0.10; $S_{\text{BET-0.3}}$, $p/p^0 = 0.05$–0.30 (Gregg and Sing 1982); $W_0(N_2)$, micropore volume, Dubinin-Radushkevich equation (Dubinin 1975)

[b] CO_2 isotherm at 0 °C: $W_0(CO_2)$, micropore volume, Dubinin-Radushkevich equation (Dubinin 1975)

[c] Mercury porosimetry: V_{ma}, macropore volume (cumulative pore volume, V_{cu}, at $r = 250$ Å, $r =$ pore radius); V_{me}, mesopore volume (V_{cu} at $r < 20$ Å–V_{ma})

[d] Helium and mercury densities (ρ_{He}, ρ_{Hg}): $V_T = 1/\rho_{\text{Hg}} - 1/\rho_{\text{He}}$

Table 3 Surface analysis of the ACs[a]

Sample codes	pH_{zpc}	Oxygen surface groups (meq/g)					Basic groups (meq/g)
		Carboxyl	Lactone	Hydroxyl	Carbonyl	Total	Total
P-0.64-400	n-d	0.64	0.05	0.46	2.40	3.55	n-m
P-3.44-400	n-d	0.34	0.12	0.43	1.81	2.70	n-m
P-3.44-500	2.7	0.66	n-m	0.29	n-m	0.95	n-m
Z-1-500	n-d	0.76	n-m	0.66	n-m	1.42	n-m
Z-4-500	6.6	0.15	0.14	0.15	0.78	1.22	0.25
Z-4-800	7.9	0.74	n-m	0.59	n-m	1.33	0.71
K-1-800	5.9	0.06	0.30	0.59	0.61	1.56	2.66
K-3-500	n-d	0.14	0.21	0.68	0.96	1.99	0.55
K-3-800	n-d	0.36	0.02	0.39	0.55	1.32	2.55
K-3-900	6.7	0.06	n-m	0.12	1.95	2.13	2.62

[a] n-d: non-determined. n-m: non-measurable

added first. A smaller mass of the K carbons was used as the adsorption of mercury was higher for these adsorbents. Then 25 mL of adsorptive solution containing either $HgCl_2$ alone (10^{-4} mol/L) or $HgCl_2$ (10^{-4} mol/L) together with $ZnCl_2$ (10^{-4} mol/L) and $CdCl_2$ (10^{-4} mol/L) (all metal chlorides, analytical reagents, Merck) were brought into contact with the carbonaceous adsorbent. The initial solution pH (≈ 5) was not adjusted to avoid adsorptive/acid-base competition effects for the surface active sites of the adsorbent. The tubes were mounted in a thermostatic shaker bath containing water at 25 °C and maintained under steady shaking of 50 oscillations per min for different times ranging from 0 to 480 h. After that, the supernatant liquid was separated from the residual carbonaceous product by filtration and analyzed by effecting absorbance measurements at 231 nm, using an UV-V Shimadzu PC-3101 equipment, as at this wavelength value the Cl_4Hg^{2-} complex anion, which is formed between HCl and $HgCl_2$ in aqueous solution, absorbs radiation. The

Table 4 Kinetic and equilibrium data

Sample	Pseudo-first order kinetic model			Pseudo-second order kinetic model				q'_e[b] ($\times 10^5$) (mol/g)	AP[d]
	k_1[a] ($\times 10^3$) (1/h)	r^2	$q_{e,1}$[b] ($\times 10^5$) (mol/g)	k_2[a] ($\times 10^{-3}$) (g/mol h)	r^2	t_e[c] (h)	$q_{e,2}$[b] ($\times 10^5$) (mol/g)		
Single-solute solution									
P-0.64-400	30.14	0.9460	1.65	4.56	0.9647	200	2.24	2.12	86
P-3.44-400	130.81	0.8261	0.99	36.98	0.9921	75	1.73	1.70	68
P-3.44-500	39.15	0.9687	1.30	13.86	0.9951	125	2.16	2.08	84
Z-1-500	29.48	0.9219	1.50	9.45	0.9973	250	2.37	2.36	95
Z-4-500	162.82	0.9829	1.43	40.87	0.9981	50	2.29	2.25	96
Z-4-800	226.38	0.5989	1.26	67.69	0.9973	25	2.43	2.36	98
K-1-800	28.33	0.8771	6.83	2.23	0.9988	250	18.22	18.14	73
K-3-500	12.67	0.9165	8.51	1.04	0.9977	350	17.52	17.64	71
K-3-800	894.25	0.8774	4.59	43.45	0.9999	25	20.10	19.57	79
K-3-900	33.39	0.9596	5.73	4.49	0.9993	150	21.20	21.22	85
Multi-solute solution									
P-0.64-400	11.28	0.9062	1.33	3.59	0.9728	> 450	1.67	1.71	69
P-3.44-400	11.52	0.5278	0.43	26.27	0.9966	120	1.40	1.39	57
P-3.44-500	118.37	0.9866	1.29	39.63	0.9851	50	1.74	1.78	73
Z-1-500	0.23	0.8153	1.44	5.53	0.9972	350	2.31	2.29	93
Z-4-500	104.32	0.9820	1.55	23.82	0.9962	75	2.48	2.42	98
Z-4-800	91.20	0.8628	1.15	38.36	0.9991	75	2.46	2.41	96
K-1-800	34.08	0.7057	5.58	4.98	0.9980	150	14.77	14.90	59
K-3-500	29.48	0.9610	6.55	2.76	0.9938	150	11.25	11.35	45
K-3-800	3638.74	0.9934	9.82	36.90	0.9991	25	18.27	17.52	71
K-3-900	97.65	0.9381	5.58	8.33	0.9975	50	17.10	16.82	69

[a] k_1, first order adsorption rate; k_2, second order adsorption rate

[b] q_e, amount of mercury adsorbed at equilibrium: $q_{e,1}$, pseudo first order kinetics; $q_{e,2}$, pseudo second order kinetics; q'_e, from (1)

[c] Equilibration time

[d] Adsorption percentages

amount of metal adsorbed at time t (h), q_t (mol/g), was calculated from the mass balance (1):

$$q_t = \frac{C_0 - C_t}{W} V \tag{1}$$

where C_0 (mol/L) is the initial concentration of the mercury solution, C_t (mol/L) is the concentration of the supernatant liquid at time t, V (L) is the solution volume used, and W (g) is the mass of adsorbent.

The experimental kinetic data, i.e. $C_t = f(t)$, were fitted using a pseudo-first order kinetic model (Lagergren 1898; Ho 2004) (2) and a pseudo-second order kinetic model (Ho and McKay 1998, 1999) (3):

$$\log(q_e - q_t) = \log q_e - \frac{k_1}{2.303} t \tag{2}$$

$$\frac{t}{q_t} = \frac{1}{k_2 q_e^2} + \frac{1}{q_e} t \tag{3}$$

where k_1 (1/h) and k_2 (g/mol h) are the first order and second order rate constants, respectively. Equations (1) and (2) were applied in the time interval between $t = 0$ and $t = t_e$ (i.e. the equilibration time, which was usually different for the various adsorption systems). q_e (mol/g) is the amount of mercury adsorbed at t_e. The values of k_1, k_2, r^2 (i.e., the linear correlation coefficient) and q_e (i.e. $q_{e,1}$ and $q_{e,2}$) are set out in Table 4. From the r^2 values it follows that, regardless of the series of carbons and of the number of components of the solution, the X–t data fit much better to (3) than to (2), which denotes that the adsorption process is second-order.

Using (1) as well, q'_e (mol/g) was estimated by simply replacing C_t with C_e (i.e., the equilibrium concentration). From q'_e the adsorption percentage of mercury (AP) was calculated by the expression $(q'_e/q_0) \times 100$, q_0 being the amount of mercury present in $V(L)$ per gram of adsorbent. The values thus obtained of q_e' and AP are also listed in Table 4.

3 Results

3.1 Preparation and characterization of AC

Data obtained in the preparation and textural characterization of the ACs, which have been previously reported for each activating agent separately (Olivares-Marín et al. 2006a, 2006b, 2007), are compared for the first time in the present study. As shown in Table 1, the yield of the process of preparation of AC is higher by the order P carbons > Z carbons ≫ K carbons. It varies in turn in the range 48–45%, 39–38% and 20–5%. Accordingly, the decrease produced in yield with the increase in I_R, or C_T, or both is more sensitive for the activation with KOH.

The values of S_{BET} and pore volumes (Table 2) indicate that the chemical activation of CS with H_3PO_4, $ZnCl_2$ or KOH is an effective method to prepare ACs with a wide range of pore volumes and sizes. The apparent BET surface area was calculated by applying the BET equation to two p/p^0 ranges, namely, 0.05–0.1 ($S_{\mathrm{BET\text{-}0.1}}$) and 0.05–0.03 ($S_{\mathrm{BET\text{-}0.3}}$). The significantly higher S_{BET} for Z-4-500, V_{me} for P-3.44-500, and V_{ma} and V_T for K-3-900 are worth mentioning, and also the fact that microporosity is well-developed in most of the ACs. Furthermore, the content of the narrow micropore must be high in Z-1-500, K-1-800, K-3-500 and K-3-800, as $W_0(CO_2)$ is high compared to $W_0(N_2)$ for this series of carbons. In contrast to microporosity, the development of mesoporosity is important only for a few ACs, in particular for P-3.44-400, P-3.44-500 and Z-4-500. These ACs were prepared by activation with H_3PO_4 and $ZnCl_2$, I_R being the highest. Usually, the increase in I_R or C_T also has a favorable effect on macroporosity, mainly when activating with KOH. As a result, macropore content is very high for most of the K carbons. Finally, it should be noted that, as shown by the very high V_T values, matter-free space is very large in K-3-800 and K-3-900. In brief, it can be stated that the porous structure of ACs prepared from CS by the method of chemical activation is strongly dependent on the activating agents, I_R and C_T.

The pH_{zpc} has previously been defined as the point at which surface charge is independent of ionic strength (Parks 1965) and as the pH above which the total surface of the carbon particles is negatively charged (Leon y Leon et al. 1992). For the ACs analyzed, the pH_{zpc} (Table 3) is significantly lower for the P carbon than for the Z carbons and K carbons. Accordingly, the H_3PO_4-activation product remains negatively charged in its surface at lower pHs than for the other carbons. As shown by the FT-IR spectra (Fig. 1), the content of the surface groups is much higher for both H_3PO_4-activation products. The spectrum registered for P-3.44-500, in particular, displays various strong absorption bands or shoulders which may be assigned to various bond stretching (ν) vibration modes, as follows: 3387 cm^{-1}, ν(O–H); 1693 cm^{-1}, ν(C=O); 1577 cm^{-1}, ν(C=C); 1175 cm^{-1}, ν(C–O), ν(P=O); 1001 cm^{-1}, ν(P–O), ν(O–C); 912 cm^{-1}, ν(P–O). In the case of K-3-900, the spectrum shows relatively weak bands at 3446, 1572 and 1223 cm^{-1}, which are in turn compatible with the absorption of infrared radiation owing to ν(O–H), ν(C=C) and ν(C–O) vibrations. However, no band ascribable to the ν(C=O) vibration in, for instance, carboxyl groups is registered in the aforesaid spectrum. The results obtained by Boehm's titration method (Boehm's, 1966) (Table 3) show that the content of acidic groups (i.e., carboxylic acid, acid anhydride or lactone groups) is very low for the KOH-activation carbons and much higher for the H_3PO_4-activation carbons. The opposite applies to the basic groups (i.e., carbonyl, ether, and so on, structures).

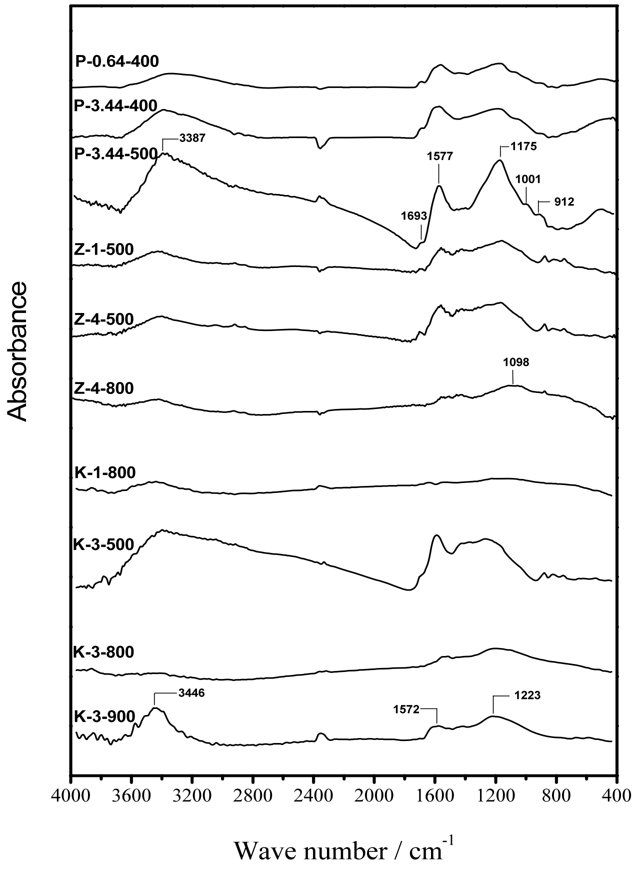

Fig. 1 FT-IR spectra of the ACs

3.2 Kinetics of mercury adsorption

Figures 2, 3, and 4 depict the variation of C_t with t separately for the three series of ACs. For the AC/single solute

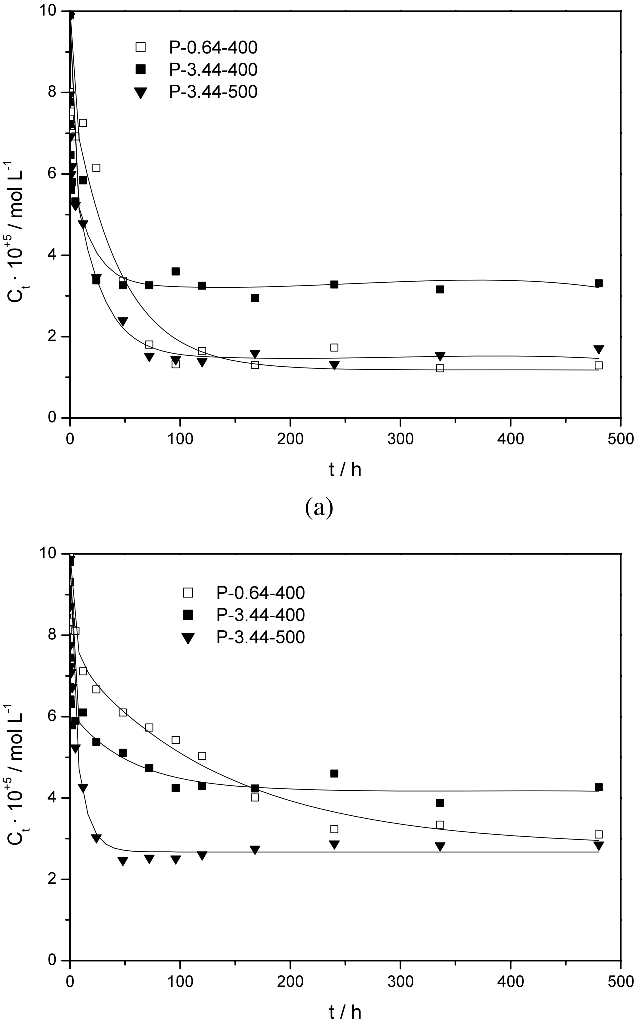

(a)

(b)

Fig. 2 Kinetics of mercury adsorption: Series P; (**a**) single component system, (**b**) multi-component system

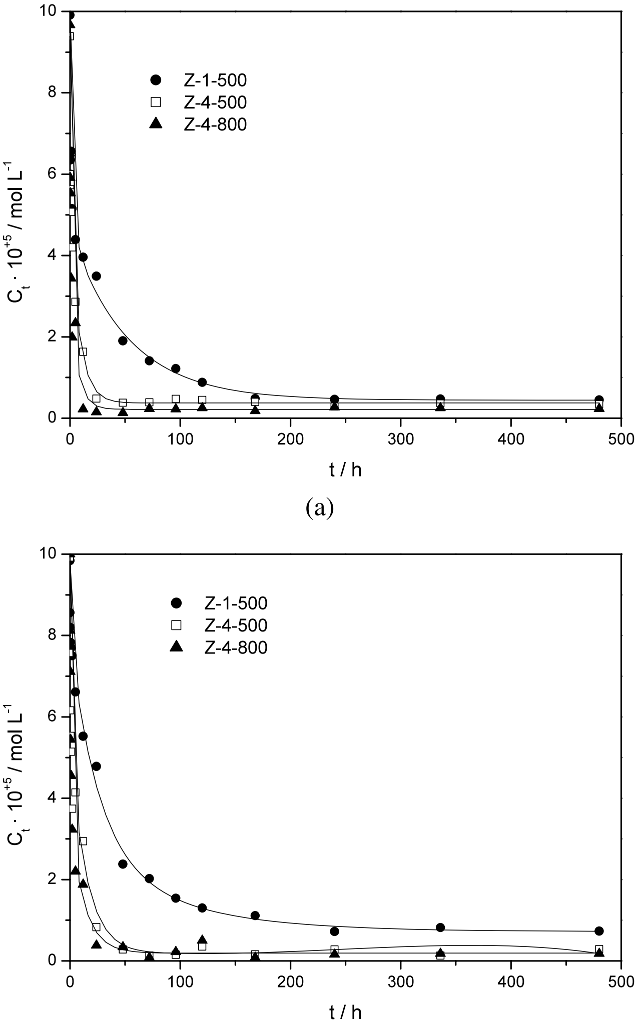

(a)

(b)

Fig. 3 Kinetics of mercury adsorption: Series Z; (**a**) single component system, (**b**) multi-component system

solution-adsorption systems, the slope of the descending branch in the C_t-t plots suggests that the kinetics of the adsorption process of mercury is slower for P-0.64-400, Z-1-500, K-1-800, and K-3-500. This was expected, since these ACs were prepared with a small degree of activation, i.e. using either a low I_R, or C_T, or both. For such adsorption systems, t_e ranges from 200 to 350 h (Table 4). The aforesaid ACs usually possess a poorly developed mesoporosity and the macropore content is also low for some products (see Table 2). In addition, the micropores present in the carbons are narrow pores which may contain constrictions. In view of these textural properties of the carbons it is likely that their porous structure had a strong influence on the diffusion of adsorptive solution in pores of the adsorbent and the kinetics of the adsorption process.

With a greater degree of activation in the preparation of ACs, the kinetics of the adsorption process is faster. Thus, $k_2 \times 10^{-3}$ g/mol h is higher for P-3.44-400 (36.98), Z-4-800 (67.69) and K-3-800 (43.45). Furthermore, t_e is 75 h for P-3.44-400 and 25 h for Z-4-800 and K-3-800. From these results it becomes clear that, by using CS as an AC precursor, an AC can be prepared that permits a rapid removal of mercury from aqueous solution, in particular when such an AC is obtained by activating with $ZnCl_2$ or KOH. On the other hand, k_2 rises with the increase in I_R and C_T for the Z carbons. This also applies to the P carbons and K carbons, though only for C_T.

The kinetics of the adsorption process of mercury from the single-solute aqueous solution is slower for P-3.44-500 than for P-3.44-400 and for K-3-900 than for K-3-800, in spite of the better developed porosity in the regions of micro-, meso- and macropores for P-3.44-500 and K-3-900 (Table 2). Accordingly, factors other than the porous structure of the ACs influence the adsorption kinetics of mer-

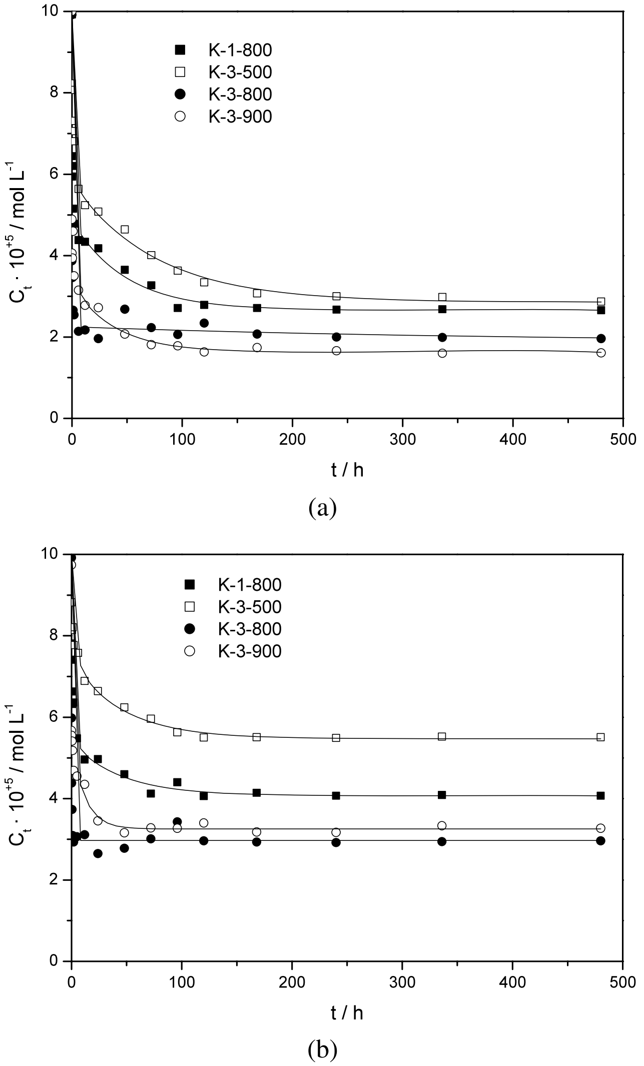

Fig. 4 Kinetics of mercury adsorption: Series K; (**a**) single component system, (**b**) multi-component system

cury. Probably one such factor is associated with the surface chemistry of the carbons. The surface groups may render difficult the access of the adsorptive to the adsorption sites because of steric effects. These would be enhanced owing to the hydrophilic character of such groups and therefore to the increase produced in their size because of the uptake of water molecules. This interpretation of the results is in line with the higher content of surface groups for P-3.44-500 than for P-3.44-400 and for K-3-900 than for K-3-800, as clearly shown by the FT-IR spectra (Fig. 1). Also, the total content of oxygen surface groups is higher for K-3-900 than for K-3-800 (Table 3). Since it is lower for P-3.44-500 than P-3.44-400, a fraction of the surface functionalities present in these ACs may not be amenable to Boehm's method, used in their quantification. The aforesaid fraction should be much higher for P-3.44-500 than for P-3.44-400, in accordance with the FT-IR results. In fact, as seen above, the H_3PO_4 activation products not only contain oxygen surface groups but also phosphorus surface groups.

In the experiments of mercury adsorption from the multi-solute solution, not only was $HgCl_2$ present in the adsorptive solution but also $ZnCl_2$ and $CdCl_2$. Furthermore, the concentration of the three metal chlorides was the same in the initial solution. Before discussing the results obtained in the study of the kinetics of the adsorption process of mercury in the presence $ZnCl_2$ and $CdCl_2$, one must consider the chemical species actually present in the adsorptive solution that was brought into contact with the adsorbent. In accordance with the literature (Bailar et al. 1973), $HgCl_2$ in aqueous solution exists mostly as undissociated $HgCl_2$ molecules and also as small amounts of $HgCl^+$ and $HgCl_3^-$, very small amounts of Hg^{2+} and $HgCl_4^{2-}$, and hydrolysis products such as Hg(OH)Cl. As far as $ZnCl_2$ is concerned, at concentrations of less than 1M, the compound almost entirely dissociated into Zn^{2+} and Cl^-; more concentrated solutions appear to contain linear $ZnCl_2$, tetrahedral $ZnCl_4^{2-}$ and possibly planar $ZnCl_3^-$ ions. Although aqueous solutions of $CdCl_2$ behave as though they contained a large proportion of undissociated $CdCl_2$ molecules, it would appear from conductivity and spectral studies that this is a result of the high tendency to form auto-complexes, i.e. to give species of the form $CdCl^+$, $CdCl_3^-$, $CdCl_4^{2-}$, etc. In brief, in dilute aqueous solution, $HgCl_2$ is largely found as a molecular substance, $ZnCl_2$ as Zn^{2+} and Cl^-, and $CdCl_2$ as $CdCl_2$ molecules or complex ions.

From Figs. 2, 3, and 4 and data in Table 4 it follows that the presence of $ZnCl_2$ and $CdCl_2$ in the $HgCl_2$ solution markedly influences the kinetics of the adsorption process of mercury. Usually it is decelerated for the series P and Z. Regardless of the influence of the solution composition on its viscosity, the multi-solute solution rather than the single-solute solution will be less mobile in the pores of the adsorbent owing to the higher concentration of chemical species with a higher charge at the liquid/solid interface, as a result of the formation of the so-called electrical double layer (i.e. one of the layers would be made up of the surface groups of the adsorbent), and hence to the fact that the interactions occurring in this interface between the surface groups and the species will be more numerous and stronger. This also applies to the bulk of the solution as in this case not only dipole (water molecules)-dipole ($HgCl_2$ molecules) interactions, as with the single-solute solution, but also dipole (water molecules, $HgCl_2$ molecules, $CdCl_2$ molecules)-ion (Zn^{2+}, cadmium complex ions, etc.) interactions are possible. The $HgCl_2$ molecular dipole, before becoming adsorbed at the last stage of the adsorption process, had to move through a layer of higher charge ions situated closer to the pore wall, because of the electrical double layer. As a result, the displacement of the adsorptive towards the surface active sites of the adsorbent should be more difficult for the multi-solute solution, and this should decelerate the adsorption process of mercury. In connection with these statements it is pertinent to recall here that the net charge on the adsorbent surface, and therefore the conformation of the electrical double layer, will depend on the relative values of the pH_{zpc} for the adsorbent (Table 3) and pH of the adsorptive solution (∼5). On the other hand, for the series P and Z the kinetics is faster with the increase in the degree of activation of the carbons, which indicates that the effect of the interactions at the electrical double layer becomes weaker when the adsorbent contains wider pores, as expected.

For most K carbons, unlike for P and Z carbons, the kinetics is significantly faster for the multi-solute solution. K carbons contain high contents of narrow micropores (see the textural data in Table 2) at the entrances of which, due to the greater presence of unsaturated residual valences, oxygen surface groups may concentrate, which may then hinder access to such pores. When the multi-solute solution is used, owing to the large degree of interaction existing in the pore mouths, it is possible that the water molecules present in the uptaken state are affected and that this facilitates access to the inner porosity of the carbons, where most of their surface area concentrates and the adsorption to a large extent occurs. If so, the oxygen surface groups would play an important role in controlling the diffusion of the adsorptive solution and also the kinetics of the process, which would then be favored with respect to the single-solute solution as in this instance the interactions between the adsorptive molecules and the water molecules uptaken on the oxygen surface groups would be weaker. This interpretation of the results is supported by the fact that the only carbon of the series K for which the adsorption kinetics of mercury is faster for the single-solute solution (i.e. K-3-800) possesses the lowest total content of oxygen surface groups (Table 3). On the other hand, it is also possible that in narrow micropores the electrical double layers situated in opposite pore walls, owing to their mutual influence, suffer a distortion that leads to a decreased number and strength of the interactions at the liquid/solid interface, the liquid phase becoming then more mobile in the pore.

3.3 Adsorption of mercury at equilibrium

The values of $q_{e,1}$, $q_{e,2}$ and q'_e (Table 4) show that $q_{e,1} \ll q_{e,2} \approx q'_e$. Also, as expected, $q_{e,2}$ and q'_e vary by the order K carbons ≫ Z carbons > P carbons, regardless of the solution composition. As a guide, the plot of $q_{e,2}$ against S_{BET} for the multi-solute solution is shown in Fig. 5. $q_{e,2}$ slightly increases with $S_{\mathrm{BET\text{-}0.1}}$ or $S_{\mathrm{BET\text{-}0.3}}$ for the K carbons (notice that the slope of the straight line is only a little greater for $S_{\mathrm{BET\text{-}0.3}}$), whereas for the P carbons and Z carbons $q_{e,2}$ is practically insensitive to the S_{BET} increase. Accordingly, it is clear that factors other than the development of surface area must be responsible for the increase in q_e with the degree of activation reached in their preparation.

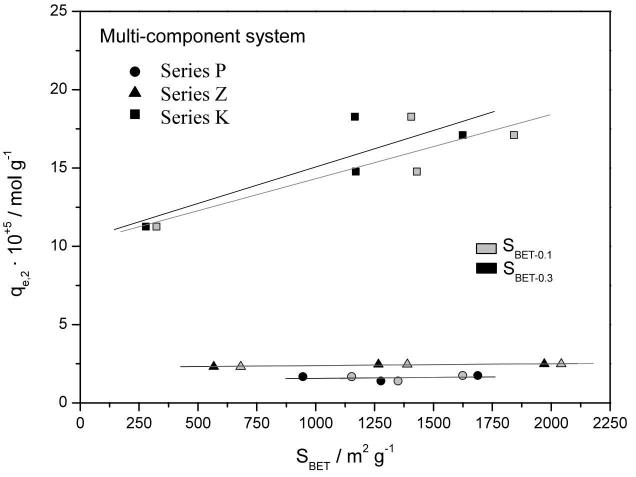

Fig. 5 Plots of $q_{e,2}$ versus S_{BET} for the multi-solute solution

AP (Table 4) is significantly higher for the Z carbons than for the P carbons and K carbons. For the Z carbons, AP values are above 90. Furthermore, the differences between the AP values obtained for both adsorptive solutions are very small. These results must be highlighted as they indicate that there is practically no competition between mercury and the other chemical species of the multi-solute solution for the adsorption sites. Therefore, it is likely that mercury adsorbs specifically on active sites of the adsorbent.

The mercury chloride molecule possesses two bond dipoles with their positive charge located on the mercury atom and with their negative charge situated on each of the chlorine atoms. The concentration of positive charge on the mercury atom suggests that $HgCl_2$ becomes adsorbed on the surface of the carbons by acid-basic interactions in which $HgCl_2$ behaves as an acid. This statement is supported by the fact that the amounts of mercury adsorbed by the carbons of the three series, regarded in each case as a whole, accord well with the contents of the basic groups (Table 3).

The preferential adsorption of mercury on active sites of the adsorbent may be facilitated by the weaker dipole (solvent molecules)-dipole (adsorptive, $HgCl_2$ molecule) interactions than the dipole (solvent molecules)-ion (Zn^{2+} and Cd^{2+} species) interactions in the bulk of the solution, which would speed up the displacement of $HgCl_2$ towards the surface adsorption sites and their coverage by the adsorbate. It has also been previously reported (Boehm 2002) that the surface basicities of carbons due to π electrons of the exposed graphene layers (Boehm and Voll 1970; Leon y Leon et al. 1992; Montes-Morán et al. 1998) and to pyrone-type structures on the edges of the polyaromatic layers are weak (Voll and Boehm 1971). Accordingly, the $HgCl_2$ molecule may interact preferably with such basic sites since the other metal species present in the solution, owing to the higher charge, must behave as stronger acids in the acid-base process, which as a last resort leads to the adsorption of $HgCl_2$.

4 Conclusion

Using CS as a precursor, three series of ACs were prepared by chemical activation with H_3PO_4 (series P), $ZnCl_2$ (series Z) or KOH (series K). The carbons were characterized from the physicochemical standpoint and used as adsorbents of mercury from a single solute ($HgCl_2$) solution and from a three-solute ($HgCl_2$, $ZnCl_2$, $CdCl_2$) solution, without pH adjustment. The kinetics of the adsorption process of mercury as $HgCl_2$ is faster for ACs that possess a well-developed porous structure made up of large size pores. The surface groups of the carbons play an outstanding role in the adsorption kinetics of mercury, by influencing the diffusion of the adsorptive solution in pores of the adsorbent. $k_2 \times 10^{-3}$ is higher by the order Z-4-800 (67.69 g/mol h) > K-3-800 (43.45 g/mol h) > P-3.44-400 (36.98 g/mol h). The presence of zinc and cadmium in the mercury solution slows down the adsorption of mercury for the P carbons and Z carbons and speeds it up for the K carbons. Adsorption of mercury is much higher for the K carbon than for the P and Z carbons. This has been connected with the higher content of basic groups for the K carbons. Competition effects of zinc and cadmium to the adsorption of mercury are practically negligible for the Z carbons. Accordingly, mercury adsorbs in a specific manner on surface active sites of these adsorbents, which is well in agreement with the different molecular/ionic character of the metal chlorides used in the present study.

Acknowledgements Financial support from Ministerio de Educación y Ciencia (MEC) (project BQU2002-03600) is gratefully acknowledged by the authors.

References

Bailar, J.C., Emeléus, H.J., Nyholm, R., Trotman-Dickenson, A.F. (eds.): Comprehensive Inorganic Chemistry, vol. 3. Pergamon, Oxford (1973)

Bansal, R.C., Donnet, J.-B., Stoeckli, F.: Active Carbon. Dekker, New York (1988)

Boehm, H.P.: Chemical identification of surface groups. In: Eley, D.D., Pines, H., Weisz, P.B. (eds.) Advances in Catalysis, vol. 16, pp. 179–274. Academic Press, New York (1966)

Boehm, H.P.: Surface oxides on carbon and their analysis: a critical assessment. Carbon **40**, 145–149 (2002)

Boehm, H.P., Voll, M.: Basische Oberflachenoxide auf Kohlenstoff—I. Adsorption von Sauren. Carbon **8**, 227–240 (1970)

Brunauer, S., Emmet, P.H., Teller, E.: Adsorption of gases in multimolecular layers. J. Am. Chem. Soc. **60**, 309–319 (1938)

Clarkson, T.W.: Mercury. In: Sarkar, B. (ed.) Heavy Metals in the Environment, pp. 457–503. Dekker, New York (2002)

Dubinin, M.M.: Physical adsorption of gases and vapors in micropores. In: Danielli, J.F., Rosenberg, M.D., Cadenhead, D.A. (eds.) Progress in Surface and Membrane Science, vol. 9, pp. 1–70. Academic Press, New York (1975)

Durán-Valle, C., Gómez-Corzo, M., Pastor-Villegas, J., Gómez-Serrano, V.: Study of cherry stones as raw material in preparation of carbonaceous adsorbents. J. Anal. Appl. Pyrolysis **73**, 59–67 (2005)

Gómez-Serrano, V., Macias-Garcia, A., Espinosa-Mansilla, A., Valenzuela-Calahorro, C.: Adsorption of mercury, cadmium and zinc from aqueous solution on heat-treated and sulphurized activated carbon. Water Res. 32(1–4) (1998)

Gómez-Serrano, V., Piriz-Almeida, F., Durán-Valle, C.J., Pastor-Villegas, J.: Formation of oxygen structures by air activation. A study by FT-IR spectroscopy. Carbon **37**, 1517–1528 (1999)

Gómez-Serrano, V., Fernández-González, M.C., Alexandre-Franco, M., Macías-García, A.: Optimizing the application of infrared spectroscopy for the study of carbonaceous adsorbents. Ann. Chim. **30**(1), 77–94 (2005)

Gregg, S.J., Sing, K.S.W.: Adsorption, Surface Area and Porosity. Academic Press, London (1982)

Ho, Y.S.: Citation review of Lagergren kinetic rate equation on adsorption reactions. Scientometrics **59**, 171–177 (2004)

Ho, Y.S., McKay, G.: Kinetic models for the sorption of dye from aqueous solution by wood. Process Saf. Environ. Prot. **76B**, 183–191 (1998)

Ho, Y.S., McKay, G.: Pseudo-second order model for sorption processes. Process Biochem. **34**, 451–465 (1999)

Ho, T.C., Kobayashi, N., Lee, Y., Lin, J., Hopper, J.R.: Experimental and kinetic study of mercury adsorption on various activated carbons in a fixed-bed adsorber. Environ. Eng. Sci. **21**, 21–27 (2004)

Hsi, H.-C., Rood, M.J., Rostam-Abadi, M., Chen, S., Chang, R.: Mercury adsorption properties of sulfur-impregnated adsorbents. J. Environ. Eng. **128**, 1080–1089 (2002)

Lagergren, S.: About the theory of so called adsorption of soluble substances. K. Sven. Vetensk. Handlingar **24**, 1–39 (1898)

Leon y Leon, C., Solar, J.M., Calemma, V., Radovic, L.R.: Evidence for the protonation of basal plane sites on carbon. Carbon **30**(5), 797–811 (1992)

Li, Y.H., Lee, C.W., Gullett, B.K.: Importance of activated carbon's oxygen surface functional groups on elemental mercury adsorption. Fuel **82**, 451–457 (2003)

Lopez-Ramon, M.V., Stoeckli, F., Moreno-Castilla, C., Carrasco-Marin, F.: On the characterization of acidic and basic surface sites on carbons by various techniques. Carbon **37**, 1215–1221 (1999)

Montes-Morán, M.A., Menéndez, J.A., Fuente, E., Suárez, D.: Contribution of the basal planes to carbon basicity: An ab initio study of the H_3O^+-π interaction in cluster models. J. Phys. Chem. B **102**(29), 5595–5601 (1998)

Nabais, J.V., Carrott, P.J.M., Carrott, M.M.L.R., Belchior, M., Boavida, D., Diall, T.I., Gulyurtlu, I.: Mercury removal from aqueous solution and flue gas by adsorption on activated carbon fibres. Appl. Surf. Sci. **252**, 6046–6052 (2006)

Newcombe, C.D., Hayes, R., Drikas, M.: Granular activated carbon: importance of surface properties in the adsorption of naturally occurring organics. Colloids Surf. A **78**, 65–71 (1993)

Olivares-Marín, M., Fernández-González, C., Macías-García, A., Gómez-Serrano, V.: Preparation of activated carbons from cherry stones by activation with potassium hydroxide. Appl. Surf. Sci. **252**, 5980–5983 (2006a)

Olivares-Marín, M., Fernández-González, C., Macías-García, A., Gómez-Serrano, V.: Preparation of activated carbon from cherry stones by chemical activation with $ZnCl_2$ Appl. Surf. Sci. **252**, 5967–5971 (2006b)

Olivares-Marín, M., Fernández-González, C., Macías-García, A., Gómez-Serrano, V.: Porous structure of activated carbon prepared from cherry stones by chemical activation with phosphoric acid. Energy. Fuel **21**(5), 2949–2942 (2007)

Pardo-Botello, R., Fernández-González, C., Pinilla-Gil, E., Cuerda-Correa, E.M., Gómez-Serrano, V.: Adsorption kinetics of zinc in multicomponent ionic systems J. Colloid Interface Sci. **277**, 292–298 (2004)

Pardo-Botello, R., Pinilla-Gil, E., Fernández-González, C., Gómez-Serrano, V.: Monotoring of Zn(II) and Cd(II) adsorption on activated carbon from aqueous multicomponent solutions by differential pulse polarography (DPP). Int. J. Environ. Anal. Chem. **85**, 1051–1063 (2005)

Parks, G.A.: The aqueous surface chemistry of oxides and complex oxide minerals. Chem. Rev. **65**, 177 (1965)

Pulido, L.L., Hata, T., Imamura, Y., Ishihara, S., Kajimoto, T.: Removal of mercury and other metals by carbonized wood powder from aqueous solutions of their salts. J. Wood Sci. **44**, 237–243 (1998)

Valenzuela Calahorro, C., Macias Garcia, A., Bernalte Garcia, A., Gómez Serrano, V.: Study of sulfur introduction in activated carbon. Carbon **28**, 321–335 (1990)

Voll, M., Boehm, H.P.: Basische Oberflachenoxide auf Kohlenstoff—IV. Chemische Reaktionen zur Identifizierung der Oberflachengruppen. Carbon **9**, 481–488 (1971)

Yardim, M.F., Budinova, T., Ekinci, E., Petrov, N., Razvigorova, M., Minkova, V.: Removal of Mercury (II) from aqueous solution by activated carbon obtained from furfural. Chemosphere **52**, 835–841 (2003)

Zelikoff, J.T., Thomas, P.T.: Inmunotoxicology of Environmental and Occupational Metals. Taylor & Francis, London (2005), pp. 131–160

Zhang, F.-S., Nriagu, J.O., Itoh, H.: Mercury removal from water using activated carbons derived from organic sewage sludge. Water Res. **39**, 389–395 (2005)